ARCHIVES OF BIOCHEMISTRY AND BIOPHYSICS
Vol. 356, No. 2, August 15, pp. 214–228, 1998
Article No. BB980756

Mechanism of Mammalian Soluble Epoxide Hydrolase Inhibition by Chalcone Oxide Derivatives[1]

Christophe Morisseau, Gehua Du, John W. Newman, and Bruce D. Hammock[2]
Department of Entomology and Department of Environmental Toxicology, University of California, Davis, California 95616

Received February 6, 1998, and in revised form May 8, 1998

A series of substituted chalcone oxides (1,3-diphenyl-2-oxiranyl propanones) and structural analogs was synthesized to investigate the mechanism by which they inhibit soluble epoxide hydrolases (sEH). The inhibitor potency and inhibition kinetics were evaluated using both murine and human recombinant sEH. Inhibition kinetics were well described by the kinetic models of A. R. Main (1982, *in* Introduction to Biochemical Toxicology, pp. 193–223, Elsevier, New York) supporting the formation of a covalent enzyme–inhibitor intermediate with a half-life inversely proportional to inhibitor potency. Structure–activity relationships describe active-site steric constraints and support a mechanism of inhibition consistent with the electronic stabilization of the covalent enzyme–inhibitor intermediate. The electronic effects induced by altering the ketone functionality and the *para*-substitution of the phenyl attached to the epoxy C_1 (i.e., the α-carbon) had the greatest influence on inhibitor potency. The direction of the observed influence was reversed for the inhibitory potency of glycidol (1-phenyl-2-oxiranylpropanol) derivatives. Recent insights into the mechanism of epoxide hydrolase activity are combined with these experimental results to support a proposed mechanism of sEH inhibition by chalcone oxides.

Key Words: **epoxide hydrolases; chalcone oxides; structure–activity relationship; inhibition kinetics.**

Epoxide hydrolases (EH[3], EC 3.3.2.3) catalyze the hydrolysis of epoxides or arene oxides to their corresponding diols by the addition of water (1). Several members of this ubiquitous enzyme subfamily have been described based on substrate selectivity and subcellular localization. Mammalian EHs include cholesterol epoxide hydrolase (2), leukotriene A_4 hydrolase (3), hepoxilin hydrolase (4), microsomal epoxide hydrolase, and soluble epoxide hydrolase (5). The latter two enzymes have been extensively studied and found to have broad and complementary substrate selectivity (5). The microsomal and soluble forms are known to detoxify mutagenic, toxic, and carcinogenic xenobiotic epoxides (6, 7) and are involved in physiological homeostasis (11). Soluble epoxide hydrolase (sEH) is involved in the metabolism of oxylipins, including epoxides of arachidonic (8, 9) and linoleic acids (10), which are mediators of vascular permeability (11). Epoxides of olefinic lipids generated *in vivo* by enzymatic (11, 12) and auto-oxidative processes (13) have been found in association with physiological dysfunctions.

Urinary arachidonate diols are known modulators of renal water retention that are elevated in association with pregnancy-induced hypertension (11), while epoxy linoleate or leukotoxin-derived diols induce nitric oxide synthase-mediated (19) and endothelin-1-mediated (14) inflammatory responses, perturbing membrane permeability and calcium homeostasis (10). Micromolar concentrations of epoxidized linoleate have been reported in association with inflammation and hypoxia (12, 15, 16). These leukotoxin concentrations

[1] This work was supported in part by NIEHS Grant R01-ES02710, NIEHS Center for Environmental Health Sciences Grant 1P30-ES05707, and UC Davis EPA Center for Ecological Health Research Grant CR819658.

[2] To whom correspondence should be addressed at Departments of Entomology and Environmental Toxicology, University of California, One Shields Avenue, Davis, CA 95616. Fax: (530) 752-1537. E-mail: bdhammock@ucdavis.edu.

[3] Abbreviations used: EH, epoxide hydrolase; s, soluble; H, human; M, murine; TMS, trimethylsilane; ESI, electrospray ionization; DMDO, dimethyl dioxirane; MCPBA, *meta*-chloroperbenzoic acid; BSA, bovine serum albumin; NEP2C, 4-nitrophenyl-*trans*-2,3-epoxy-3-phenylpropyl carbonate; MR, molar refractivity; QSAR, quantitative structure–activity relationship; t-DPPO, *trans*-1,3-diphenylpropene oxide.

0003-9861/98 $25.00

depress mitochondrial respiration *in vitro* (17) and cause mammalian cardiopulmonary toxicity (12, 18, 19) *in vivo*. In cell culture, leukotoxin-mediated cytotoxicity is dependent on epoxide hydrolysis and correlates with diol concentration in the medium (20). The bioactivity of these epoxide hydrolysis products and their association with inflammation suggest that inhibition of the biosynthesis of 1,2-dihydroxy lipids may have therapeutic value. Therefore sEH is a promising pharmacological target.

EHs are members of the α/β hydrolase fold family (21). Members of this family of enzymes hydrolyze their substrates in a two-step mechanism involving the formation and hydrolysis of a covalent acyl- or alkyl-enzyme intermediate (21–24). The search for good sEH inhibitors has been actively pursued for the past 15 years (25–30). Numerous reagents which selectively modify thiols, imidazoles, and carboxyls (25–27) irreversibly inhibit sEH. Unfortunately, these agents have no therapeutic value due to their nonspecific mode of action and high working concentrations (>1 mM). Two classes of structurally similar, potent, and selective soluble epoxide hydrolase inhibitors have been described: substituted chalcone oxides (25, 28) and phenylglycidols (29, 30). While these inhibitors appear to act through interactions with the catalytic site, i.e., 1:1 stoichiometric ratio with sEH and additive inhibition, the enzyme slowly reactivates (25). In the current study we tested two hypothesized modes of inhibitor action which are not mutually exclusive. Specifically, we hypothesized that inhibition may proceed from a high-affinity reversible interaction between the inhibitor and the active site as described by Mullin and Hammock (25) and/or that a stable, yet transient, covalent enzyme intermediate is formed in a process analogous to the inhibition of organophosphates on other hydrolytic enzymes (36). Defining the mechanism by which chalcone oxides inhibit sEH will promote the rational design of soluble EH inhibitors for *in vitro* and *in vivo* use and by analogy may provide leads for designing microsomal EH inhibitors as well.

This report describes a structural and kinetic investigation of the mechanism of chalcone oxide derivatives as potent inhibitors of sEH. Numerous compounds were synthesized to investigate the effects of structural parameters on inhibition. In addition, enzyme kinetics were evaluated in the presence of a subset of these compounds to study their mechanism of action. This research was performed with recombinant human and murine soluble epoxide hydrolase (HsEH and MsEH). The mouse enzyme provided a rodent model to evaluate the use of mice for therapeutic development of HsEH inhibitors.

MATERIALS AND METHODS

Chemicals. Racemic 4-nitrophenyl-*trans*-2,3-epoxy-3-phenylpropyl carbonate was previously synthesized in this laboratory by Dietze *et al.* (31). All starting materials were purchased from Aldrich Chemicals (Milwaukee, WI) and used without further purification.

Product purification. Synthesized products were purified by silica gel column chromatography and repeated recrystallization. Purity was assessed by a combination of techniques including thin-layer chromatography (TLC), melting point determinations, and proton nuclear magnetic resonance (^{1}H NMR) spectroscopy. Isolated products were dissolved in diethyl ether, spotted beside starting materials, developed on fluorescent silica gel TLC plates (Merck, Germany), and visualized by UV quenching at 254 nm. TLCs were developed in hexane:ethyl acetate solvent systems to achieve clear separation of products from starting materials. The observation of a single, symmetrical, well-developed UV-dense spot was considered an indication of purity. Solid product purity was further assessed by melting point determinations using a Thomas–Hoover apparatus (A. H. Thomas Co., Philadelphia, PA). Finally, integrated ^{1}H NMR spectra were inspected for unassignable signals with intensities less than that of the characteristic epoxy protons.

Synthesis confirmation procedures. Purified products were structurally characterized using NMR, infrared (IR), and/or mass spectroscopy (MS). Proton and ^{13}C NMR spectra were acquired on a QE-300 spectrometer (Bruker NMR, Billerica, MA). ^{1}H NMR spectra were obtained for all compounds while ^{13}C NMR spectra were collected for definitive confirmations. Initial NMR spectra were collected in deuterated solvents containing trimethylsilane (TMS) and all chemical shifts are expressed in parts per million relative to the internal TMS. For the documentation of exchangeable protons, independent samples were dissolved in 1:1 CD_3CN:CD_3OD and rerun. IR spectra were obtained on a Mattson Galaxy Series FTIR 3000 spectrometer (Madison, WI) and characteristic absorbances were recorded. Positive-mode mass spectra were collected using either a gas or liquid chromatographic interface. Gas chromatography MS (GC/MS) analyses were performed using one of two systems equipped with a 30-m × 0.25-mm-i.d. × 0.25-μm film DB-5 capillary column (J & W Scientific, Folsom, CA), running with a 70-eV ionization energy in an electron ionization mode, and calibrated with perfluorotributylamine. The first GC/MS was a Hewlett–Packard (San Jose, CA) 5890A gas chromatograph equipped with a VG Trio-2 spectrometer controlled by a VG11-250 data system (Altrancham, England). The second GC/MS was a Varian 3400 *Cx* gas chromatograph equipped with an ITS40 ion-trap detection system (Sugar Land, TX) controlled by a DOS-compatible personal computer. Ionizable, thermally unstable products were analyzed by positive-mode electrospray ionization MS (ESI-MS) on a VG/Fisons Quatro Bio-Q LC/MS/MS (Altrancham, England) calibrated with polyethylene glycol.

Syntheses. Inhibitor structures are given in Table I–Table V and boldface numbers throughout the text refer to these compounds. Many of these compounds were synthesized by previously described methods (25, 28, 29). Thirty of the fifty synthesized compounds have not been previously tested as epoxide hydrolase inhibitors. The tested products were racemic mixtures with >95% purity based on ^{1}H NMR. All compounds yielded a single UV-dense spot by TLC and thermally stable solids had narrow melting point ranges indicating high purity. NMR, IR, and MS data supported the expected structures. Following is a description of the syntheses of several chalcone oxide analogs illustrating the synthetic pathways used. It should be noted that the epoxidation procedures used are not enantioselective, and all synthesized and purified agents are racemic. The nomenclature rules defined by the International Union of Pure and Applied Chemistry (IUPAC) were used for the systematic naming of these compounds while "common" names are used for much of the discussion.

TABLE I

Inhibition by 4-Substituted Chalcone Oxides

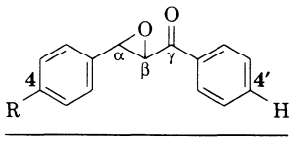

No.	R	IC_{50} (μM)[a] MsEH	HsEH
1	H	2.9 ± 0.3	0.3 ± 0.1
2	F	1.3 ± 0.3	0.3 ± 0.1
3	Br	0.7 ± 0.1	0.20 ± 0.05
4	CH_3	1.9 ± 0.2	0.36 ± 0.04
5	CH_3O	0.20 ± 0.02	0.11 ± 0.01
6	NO_2	1.8 ± 0.3	0.63 ± 0.01
7	C_6H_5	0.14 ± 0.01	0.20 ± 0.01
8	C_6H_5O	0.14 ± 0.02	0.51 ± 0.03
9	$C_6H_5CH_2O$	0.28 ± 0.02	0.23 ± 0.01
10	$(CH_3)_2CH$	0.47 ± 0.01	0.48 ± 0.01
11	n-C_7H_{15}	0.65 ± 0.01	0.48 ± 0.05
12	n-C_4H_9	0.15 ± 0.01	0.15 ± 0.01
13	COOH	>500	>500
14	$NH(CO)CH_3$	0.22 ± 0.01	0.27 ± 0.02
15	$H_2C^{O}CHCH_2O$	2.1 ± 0.2	0.29 ± 0.07

[a] Enzymes (0.13 μM MsEH or 0.26 μM HsEH) were incubated with inhibitors for 5 min in pH 7.4 phosphate buffer at 30°C prior to substrate introduction. The reported results are the IC_{50} means ± standard deviations (n = 3).

*Phenyl-3-(4-phenoxyphenyl) (2-oxiranyl) ketone (**8**).* Chalcones can be prepared by direct condensation of benzaldehydes and acetophenones in alkaline ethanol (25). The chalcone can then be directly epoxidized by a variety of methods. It should be noted that peracids produce very poor epoxidation yields in this series. 4-Phenoxychalcone was prepared by combining 30 mmol of 4-phenoxybenzaldehyde (5.9 g) and acetophenone (3.6 g) in 50 ml of absolute ethanol and stirring vigorously with 3 ml of aqueous 2 M NaOH for 2 h. The reaction mixture was refrigerated for 16 h and the resulting solid product was collected, washed with cold water, and dried. Crude solids were recrystallized from 4:1 (v/v) ethanol:benzene, yielding 6.2 g (68%) 4-phenoxychalcone as light yellow crystals. (**Caution:** benzene is a carcinogen.) Three grams of 4-phenoxychalcone (10 mmol) in 100 ml of methanol was treated with 5 ml of 30% H_2O_2 and stirred while adding 6 ml of 1 M NaOH over 30 min in an ice bath. The reaction was further stirred for 3 h at room temperature, and cold water was added. The precipitate was filtered, washed, and recrystallized from 4:1 (v/v) ethanol:benzene. The product was obtained as 2.3 g (72%) of white crystals: mp 94–95°C; FT-IR (KBr) 1660, 1605 cm^{-1}; ^1H NMR ($CDCl_3$) δ 4.06 (d, J = 1.8 Hz, 1 $H_{C\beta}$), 4.32 (d, J = 1.8 Hz, 1 $H_{C\alpha}$), 7.0 (m, 6 $H_{Aromatic}$), 7.13 (t, J = 7.5 Hz, 1 $H_{4\text{-phenoxy}}$), 7.35 (t, J = 7.5 Hz, 1 $H_{3\text{-phenoxy}}$), 7.35 (t, J = 7.5 Hz, 1 $H_{5\text{-phenoxy}}$), 7.51 (t, J = 7.2 Hz, 2 $H_{3',5'\text{-Aromatic}}$), 7.64 (t, J = 7.2 Hz, 1 $H_{4'\text{-Aromatic}}$), 8.02 (d, J = 7.2 Hz, 1 $H_{2'\text{-Aromatic}}$), 8.02 (d, J = 7.2 Hz, 1 $H_{6'\text{-Aromatic}}$); ^{13}C NMR ($CDCl_3$) δ 59.0 (C_α), 60.9 (C_β), 118.8, 119.2, 123.7, 127.3, 128.3, 128.6, 128.8, 128.8, 130.0, 133.8, 135.5, 156.6, 158.2 ($C_{Aromatic}$), 193.0 ($C_{\gamma\ ketone}$); GC/MS (% relative intensity, fragment formula) *m/z* 316 (25, $M^+ - H$, $C_{21}H_{16}O_3$), 183 (48, $C_{13}H_{11}O_3$), 105 (100, C_7H_5O), 77 (44, C_6H_5).

TABLE II

Inhibition by 4′-Substituted Chalcone Oxides

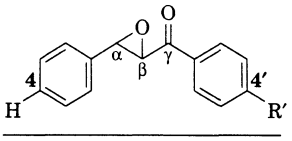

No.	R′	IC_{50} (μM)[a] MsEH	HsEH
1	H	2.9 ± 0.3	0.3 ± 0.1
16	F	1.8 ± 0.2	0.39 ± 0.09
17	Br	0.6 ± 0.1	0.22 ± 0.01
18	I	1.4 ± 0.1	0.42 ± 0.08
19	CH_3	1.7 ± 0.2	0.23 ± 0.02
20	CH_3O	0.32 ± 0.04	0.20 ± 0.04
21	NO_2	1.5 ± 0.2	0.25 ± 0.01
22	C_6H_5	1.37 ± 0.08	0.28 ± 0.03
23	$NH(CO)CH_3$	1.7 ± 0.2	0.14 ± 0.01
24	$OCH_2(CH)^{O}CH_2$	1.4 ± 0.5	0.14 ± 0.01
25	COOH	73 ± 5	144 ± 7

[a] Enzymes (0.13 μM MsEH or 0.26 μM HsEH) were incubated with inhibitors for 5 min in pH 7.4 phosphate buffer at 30°C prior to substrate introduction. The reported results are the IC_{50} means ± standard deviations (n = 3).

TABLE III

Inhibition by 4,4′-Disubstituted Chalcone Oxides

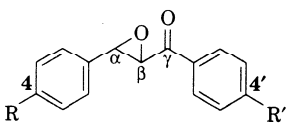

No.	R	R′	IC_{50} (μM)[a] MsEH	HsEH
1	H	H	2.9 ± 0.3	0.3 ± 0.1
7	C_6H_5	H	0.14 ± 0.01	0.20 ± 0.01
26	C_6H_5	Br	0.14 ± 0.01	0.18 ± 0.01
27	C_6H_5	CH_2Br	0.11 ± 0.02	0.16 ± 0.02
28	C_6H_5	CH_3	0.10 ± 0.01	0.19 ± 0.03
29	C_6H_5	NO_2	0.13 ± 0.02	0.16 ± 0.02
30	C_6H_5	COOH	0.08 ± 0.01	0.16 ± 0.01
31	F	COOH	103 ± 2	113 ± 3
32	COOH	F	>500	>500

[a] Enzymes (0.13 μM MsEH or 0.26 μM HsEH) were incubated with inhibitors for 5 min in pH 7.4 phosphate buffer at 30°C prior to substrate introduction. The reported results are the IC_{50} means ± standard deviations (n = 3).

*(Hydroxyimino)phenyl(3-(4-phenylphenyl) (2-oxiranyl))methane (**39**).* Chalcone oxime analogs were synthesized from chalcones with aqueous hydroxylamine hydrochloride prior to epoxidation with dimethyl dioxirane (DMDO). An ether solution containing 10 mmol 4-phenylchalcone was added to 150 ml H_2O containing an equimolar concentration of hydroxylamine hydrochloride and the mixture was stirred vigorously while a saturated solution of sodium carbonate was slowly added. The reaction temperature was maintained below 45°C. After the mixture was stirred for 1 h at room temperature, the organic phase was removed, washed with water, and dried over magnesium sulfate. The solvent was removed from the solid product by distillation and the 1-(hydroxy-

TABLE IV

Inhibition by Substituted Chalcone Oxide Derivatives

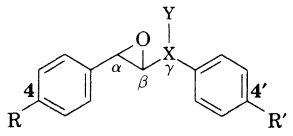

No.	R	R′	X—Y	IC_{50} (μM)[a] MsEH	HsEH
33	H	H	CH—OH	12.6 ± 0.9	22 ± 2
34	F	H	CH—OH	72 ± 16	18 ± 2
35	NO_2	H	CH—OH	3.7 ± 0.6	28 ± 1
36	C_6H_5	H	CH—OH	0.51 ± 0.04	0.72 ± 0.03
37	C_6H_5	CH_3	CH—OH	0.09 ± 0.01	0.15 ± 0.02
38	H	H	C=NOH	3.5 ± 0.5	0.29 ± 0.01
39	C_6H_5	H	C=NOH	42 ± 3	35 ± 1
40	H	H	S=O	2.3 ± 0.4	0.31 ± 0.02
41	C_6H_5	H	S=O	73 ± 3	70 ± 3
42	H	H	CH—OCH_3	103 ± 5	34 ± 1
43	C_6H_5	H	CH—OCH_3	0.48 ± 0.05	1.36 ± 0.07
44	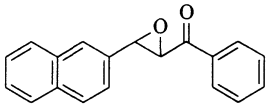			0.49 ± 0.02	0.85 ± 0.06
45	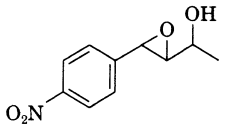			2.27 ± 0.04	18.7 ± 0.3
46	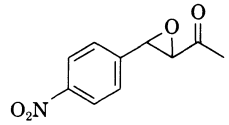			163 ± 11	269 ± 5
47	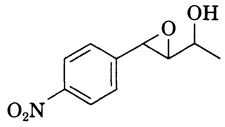			6.5 ± 0.2	39 ± 1

[a] Enzymes (0.13 μM MsEH or 0.26 μM HsEH) were incubated with inhibitors for 5 min in pH 7.4 phosphate buffer at 30°C prior to subtrate introduction. The reported results are the IC_{50} means ± standard deviations (n = 3).

imino)-1-phenyl-3-(4-phenylphenyl)prop-2-ene was purified by recrystallization from 3:2 (v/v) ethanol:water. The corresponding epoxide was prepared by oxidation with DMDO in acetone (32). The reaction was monitored by TLC. A single resolvable product was observed as starting material concentration declined. Solvents were removed by distillation to yield **39** (25%): mp thermally unstable; ^{1}H NMR ($CDCl_3$) δ 3.63 (d, J = 1.8 Hz, 1 $H_{C\beta}$), 4.06 (d, J = 1.8 Hz, 1 $H_{C\alpha}$), 7.2–7.9 (m, 14 $H_{Aromatic}$), 11.34 (s, 1 H_{Oxime}, D_2O exchangeable); ESI-MS (% relative intensity, fragment formula (M = $C_{21}H_{17}O_2N$)) *m/z* 338 (23, $(M + Na^+)^+$), 316 (83, $(M + H)^+$), 298 (100, $(M + H - H_2O)^+$); FT-IR 1592 (C=N stretch), 3438 (C=NOH) cm^{-1}.

*Phenyl(3-(4-phenylphenyl) (2-oxiranyl))methan-1-ol (**36**).* Diphenylglycidols were synthesized by reducing the respective chalcone ketone to a hydroxyl group with sodium borohydride prior to epoxidation with DMDO. One millimole (284 mg) of 4-phenylchalcone dissolved in 2.5 ml of 0.4 M methanolic $CeCl_3$ was added to a cooled suspension of 1 mmol of sodium borohydride in methanol while stirring. After 20 min, the mixture was poured into ice water and extracted three times with ether. The extracts were combined, washed with brine, dried over sodium sulfate, concentrated under a gentle stream of dry nitrogen, and purified by nitrogen-pressurized column chromatography on silica gel using a hexane: ethyl acetate (80:20 v/v) solvent system. 1-Phenyl-3-(4-phenylphenyl)prop-2-en-1-ol was obtained with a 90% yield (260 mg) and epoxidation was performed immediately with DMDO in acetone (32). The reaction was monitored by TLC. A single resolvable product was observed as starting material concentration declined. Starting materials were completely consumed in 45 min. Solvents were removed by distillation, yielding 90 mg of clear oily product

TABLE V

Calculated vs Measured Chalcone Oxide Analog MsEH IC_{50}s

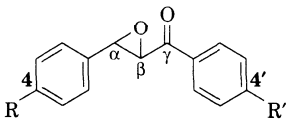

No.	R	R'	IC_{50} (μM) Calculated	Measured[a]
13	COOH	H	50	>500
30	C_6H_5	COOH	0.1	0.08 ± 0.01
31	F	COOH	2.0	103 ± 2
32	COOH	F	50	>500
48	C_6H_5	I	0.1	0.13 ± 0.01
49	CH_3O	I	0.2	0.48 ± 0.02
50	Br	CH_3O	0.4	0.27 ± 0.05

[a] 0.13 μM MsEH was incubated with inhibitors for 5 min in pH 7.4 phosphate buffer at 30°C prior to substrate introduction. The reported experimental results are the IC_{50} means ± standard deviations (n = 3).

corresponding to an approximate yield of 30%. ^{1}H NMR ($CDCl_3$) δ 2.5–2.7 (m, 1 $H_{Hydroxyl}$, D_2O exchangeable), 3.2 (d, 1 $H_{C\alpha}$), 4.1 (m, 1 $H_{C\beta}$), 4.9 (d, 1 $H_{C\gamma}$), (m, 14 $H_{Aromatic}$).

*Phenyl(3-phenyl(2-oxiranyl))methylmethyl ether (**42**).* The chalcone methyl ether analogs were synthesized from the appropriate allylic alcohol (prepared as above) prior to epoxidation with *meta*-chloroperbenzoic acid (MCPBA). Ten millimoles (2.1 g) of 1,3-diphenylprop-2-en-1-ol, 40 mg of tetrabutylammonium hydrogen sulfate, 10 ml of dichloromethane, and 1 ml 50% aqueous sodium hydroxide were mixed and stirred for 30 min at room temperature. The mixture was cooled in an ice bath and 1.3 g (10 mmol) of dimethyl sulfate (**Caution:** carcinogen) was added dropwise over a period of 1 h. The reaction mixture was stirred vigorously for 3 h at room temperature. Concentrated NH_4OH (1 ml) was then added and the mixture was stirred for 30 min, poured into double-distilled water, and extracted with 20 ml of dichloromethane. The organic phase was washed with water, dried, and evaporated. The crude product was oxidized directly with MCPBA in dichloromethane. The mixture was stirred for 3 h at room temperature and excess MCPBA was eliminated with aqueous sodium sulfite. The mixture was then filtered, washed with sodium bicarbonate, and dried over sodium sulfate. The solvent was evaporated and the epoxide product was purified by nitrogen-pressurized silica gel column chromatography using a hexane:ethyl acetate solvent system (80:20, v/v). A yellow oily product was obtained in a 45% yield (1.1 g). ^{1}H NMR ($CDCl_3$) δ 3.3 (d, 1 $H_{C\alpha}$), 3.6 (s, 3 H_{Methyl}), 4.0 (m, 1 $H_{C\beta}$), 5.1 (d, 1 $H_{C\gamma}$), 7.2–7.8 (m, 10 $H_{Aromatic}$).

Enzyme purification. Recombinant mouse sEH and human sEH were produced in a baculovirus expression system as previously reported (33, 34). The expressed proteins were purified from cell lysate by affinity chromatography (35). Protein concentration was quantified using the Pierce BCA assay (Pierce, Rockford, IL) using bovine serum albumin (BSA) as the calibrating standard. The preparations were at least 97% pure as judged by sodium dodecyl sulfate–polyacrylamide gel electrophoresis and scanning densitometry. No detectable esterase or glutathione transferase activity, which can interfere with this sEH assay, was observed (31).

IC_{50}[4] assay conditions. The IC_{50} for each inhibitor was determined by the spectrophotometric assay of Dietze *et al.* (31) using racemic 4-nitrophenyl-*trans*-2,3-epoxy-3-phenylpropyl carbonate (NEP2C; mp 72–73°C) as substrate. In a styrene 96-well microplate, 20 μl of enzyme preparation and 2 μl of the inhibitor solution in dimethyl formamide ($[I]_{Final}$, 0.05 to 500 μM) were added to 180 μl of sodium phosphate buffer (0.1 M, pH 7.4) containing 0.1 mg/ml of BSA (BSA does not affect results in concentrations of 0 to 0.5 mg/ml). The mixture was incubated at 30°C for 5 min. These conditions allow maximal inhibition with little enzyme reactivation. A substrate concentration of 40 μM was then obtained by adding 4 μl of a 2 mM solution. Activity was assessed by measuring the appearance of the 4-nitrophenolate at 405 nm at 30°C for 1 min (Spectramax 200; Molecular Device, Inc., Sunnyvale, CA). Assays were performed in quadruplicate. By definition, the IC_{50} is the concentration of inhibitor which reduces enzyme activity by 50%. IC_{50} was determined by regression of at least five datum points with a minimum of two points in the linear region of the curve on either side of the IC_{50}. The curve was generated from at least three separate runs, each in quadruplicate, to obtain the standard deviation in Tables I–IV. In at least one run, compounds of similar potency were included to ensure rank order.

Kinetic assay conditions. The kinetic constant determinations were accomplished using the two-step organophosphate cholinesterase inhibition model described by Main (36). Inhibitor concentrations between 0 and 2.5 μM were used and measurements were made in the presence of excess substrate ($[S]_{Final}$, 40 μM). The enzyme:inhibitor dissociation constant (K_d) and the rate of enzyme–inhibitor covalent complex formation (k_2) were calculated from activity measurements at 0, 5, and 10 s post-inhibitor introduction. Under these conditions, less than 10% of the inhibitor was bound to the enzyme. The rates of deacylation and product release (k_3) were calculated from enzyme activities in 1:1 enzyme:inhibitor mixtures between 1–20 min post-inhibitor introduction.

Structure–activity relationship analysis. All substituent constants came from the extensive compilation of Hansch and Leo (37). For the molar refractivity (MR), we used a base of 0.1 for protons. Multiple regression analysis of the inhibition potency ($-\log(IC_{50})$) of the 4- and 4'-substituted chalcone oxides on the mouse and human sEH were obtained using Sigma-Plot v2.0 (Jandel Scientific, San Rafael, CA) and Excel v7.0 (Microsoft, Seattle, WA). Combinations of up to three free-energy parameters for each position were investigated. The F test, which uses the ratio of the regression sum of squares to the residual sum of squares as a fit criterion (α = 0.05), was used to determine the confidence of adding parameters to multiple regression equations. Standardized regression coefficients were calculated to establish the rank order of independent variable influence on inhibitory potency.

RESULTS

Enzyme assay optimization. The spectrophotometric assay used for the kinetic study provided continuous and rapid (1 min) data collection. Reactions were executed at 30°C to minimize spontaneous hydrolysis of the substrate while maintaining high enzyme activity. Recombinant MsEH and HsEH displayed pH optimums of 7.4 and 7.6, respectively, with the spectral substrate. Both wild-type and recombinant sEH dis-

[4] By convention IC_{50} describes the binding of reversible inhibitors, not irreversible inhibitors like chalcone oxides. However, IC_{50} is used here to describe relative inhibitor potencies under the assay conditions described.

play similar pH optimums with other substrates (5, 7, 38), and we have failed to demonstrate a difference in enzyme kinetics between the wild-type and the recombinant enzymes (5). All assays were run at pH 7.4 (optimal for MsEH and 90% maximal HsEH activity) and found to be linear with respect to time up to an optical density (OD) ≥0.2 at 405 nm and enzyme concentrations of 0 to 25 μg protein/ml. Data in the linear range for both protein concentrations and inhibition times were used for IC_{50} and kinetic studies. The K_ms for MsEH and HsEH were 5.8 and 3.6 μM, respectively, under these conditions. Since the selected kinetic model requires high substrate to enzyme concentrations, 40 μM NEP2C (i.e., ~10 times K_m) was used during inhibition assays. The MsEH k_{cat} (19.2 s^{-1}) was twofold higher than that of HsEH (9.2 s^{-1}), in agreement with earlier observations using several substrates (38). A k_{cat}/K_m of approximately 3 $\mu M^1\ s^{-1}$ was calculated for both enzymes. Therefore 8 and 16 μg/ml of MsEH and HsEH, respectively, were used, producing ~100 mOD min^{-1} for both enzyme assays.

Enzyme inhibition. IC_{50}s provided relative inhibitory potency of the synthesized chalcone oxides (Table I–Table IV) and directed the selection of compounds for kinetic characterization. While the results were similar for each enzyme, MsEH was more sensitive to variations in inhibitor structure than the human enzyme. Substitutions at the 4-position (Table I) exhibited a larger range of effects on the IC_{50} than 4′-substitutions (Table II). Chalcone oxides with small *para*-substituents (e.g., H, F, Br, CH_3—Table I vs Table II) showed less differential inhibition than those with large substituents (e.g., phenyl; **7–22**), supporting a mechanism by which both faces of smaller molecules can approach the catalytic site and impart a lack of enantiofacial selectivity. As the size of the *para*-substituent increases, differences become apparent in the potency of 4- and 4′-substituted chalcones (Table I vs Table II). Additionally, large 4-position substitutions were only weakly modulated by 4′-modifications (Table III), e.g., **7** vs **26–30,** lending further support to the existence of two nonequivalent pockets adjacent to the catalytic site (25).

Subtitutent size also affected the inhibitory potency of the γ-carbon hydroxy chalcone oxide analogs (i.e., glycidols; Table IV). With small 4-position substituents, glycidols showed potency reductions up to 70-fold (**33–1, 34–2, 35–6**) compared to the corresponding chalcone oxides. Smaller potency reductions were realized with 4-phenyl substitutions (**36–7**) while a slight increase in potency was observed with the 4-phenyl-4′-methyl substitutions (**37–28**). These opposing trends observed for chalcone oxide and glycidol derivatives IC_{50}s are consistent with earlier comparisons of 4-nitrochalcones and glycidols (29). A similar trend is observed for the tested γ-methoxy analogs (**42, 43**); however, an opposite trend was seen when the γ-carbon carbonyl functionality was replaced by either an oxime (**38, 39**) or a sulfinyl (**40, 41**). These results illustrate an interaction between the substituents of the 4-position and the γ-carbon. More severe alterations of the chalcone skeleton allowed further investigation of these interactions. The elimination of the phenyl ring substituent of the γ-carbon in the 4-nitrophenylglycidol analogs **45–47** gave IC_{50}s similar to or higher than those given by **6** and **35,** the related chalcone oxides. The γ-carbon hydroxyl-containing 4-nitro compounds, **45** and **47,** were more potent inhibitors than the corresponding ketone (**46**).

In the phenylglycidol series, enantiospecific inhibition of sEH has been described for potent derivatives. For example, the 4-nitrophenylglycidol (**47**) (*S,S*) enantiomer has a 500-fold greater inhibitory potency than the (*R,R*) form (29, 30). The enantiomers of 4-fluorochalcone oxide (**2**), however, are of almost identical potency (29). This observation again suggests that the chalcone oxides with no or small *para*-phenyl substitutions lack enantiofacial selectivity with the enzyme. Thus, on the chalcone oxide skeleton, the inhibitor may take position in the catalytic site to give maximal inhibition by a substituent in the γ-position while the 4-phenyl chalcone oxide is locked in a single position in which the γ-carbonyl (**7**), hydroxy (**36**), or methoxy (**43**) is an activator, but an oxime (**39**) or sulfinyl (**41**) has low potency.

Quantitative structure–activity relationship (QSAR). Multiple regression QSAR analyses relating the inhibitor potency (−log (IC_{50})) of 27 chalcone oxides and molecular free energy changes related to 4- and 4′-substituent effects on electronic (σ, $\sigma-$, $\sigma+$), hydrophobic (π), and steric (MR) parameters were performed. Structures were chosen such that free energy parameters were noncollinear ($r^2 < 0.3$). Carboxylate-containing compounds (**13, 25, 30, 31,** and **32**) were removed from the 32 chalcone oxide derivative data set (**1–32**) to avoid variability induced by the presence of both ionized and un-ionized forms. The multiple regression equations for each enzyme were developed in a stepwise fashion as described in Table VI. The structural correlations of chalcone oxide derivatives with MsEH inhibition potency produced the equation

$$\begin{aligned}-\log(IC_{50}) &= -0.42(\pm 0.18)\sigma_4^+ + 0.027(\pm 0.07)\pi_4 \\ &\quad - 0.036(\pm 0.018)\pi_4^2 + 0.85(\pm 0.16)MR_4 \\ &\quad - 0.17(\pm 0.06)MR_4^2 + 0.56(+0.21)MR_{4'} \\ &\quad - 0.21(\pm 0.09)MR_{4'}^2 + 5.55(+0.11), \\ &\quad n = 27,\ r = 0.92,\ s = \pm 0.22,\ P(F) = 0.67, \quad [1]\end{aligned}$$

TABLE VI

Stepwise Development of QSAR Eq. [1][a]

$$-\log(IC_{50}) = a + b\sigma_4^+ + c\pi_4 + d\pi_4^2 + e\mathrm{MR}_4 + f\mathrm{MR}_4^2 + g\mathrm{MR}_{4'} + h\mathrm{MR}_{4'}^2$$

a	b	c	d	e	f	g	h	n[b]	r[b]	s[b]	$P(F)$[b]
6.13	−0.75							27	0.46	0.19	>0.01
6.04	−0.69	0.16						27	0.71	0.20	0.07
5.91	−0.37	0.097		0.18				27	0.77	0.21	0.19
5.84	−0.30	−0.078	−0.062	0.48				27	0.86	0.21	0.42
5.76	−0.33	0.0085	−0.044	0.79	−0.14			27	0.88	0.22	0.56
5.64	−0.37	0.018	−0.041	0.85	−0.16	0.14		27	0.89	0.22	0.60
5.55	−0.42	0.027	−0.036	0.85	−0.17	0.56	−0.21	27	0.92	0.22	0.67

[a] Combinations of up to three free-energy parameters for each position were sequentially investigated by multiple regression analysis of the inhibition potency (−log (IC_{50})) of the 4- and 4′-substituted chalcone oxides on the mouse sEH. The F test was used to determine the confidence of adding parameters to regression equations.

[b] n, number of inhibitors included in calculation; r, correlation coefficient; s, standard deviation; $P(F)$, F test probability.

which was significant ($P < 0.05$). Values in parentheses are independent variable coefficient standard deviations.

Eighty-five percent of the correlation in chalcone oxide derivative action against the murine enzyme as determined by IC_{50} was described by this equation, which indicated optimal inhibition when $\sigma_4^+ < 0$, $\pi_4 \sim 2.0$, $MR_4 \sim 2.5$, and $MR_{4'} \sim 1.5$. The experimental versus calculated IC_{50}s for the MsEH are displayed in Fig. 1. Calculation of the standardized regression coefficients for each of the significant independent variables indicated that inhibitory potency was affected by linear free energy parameters in the order $MR_{4'} > \sigma_4^+ > MR_{4'}^2 > MR_4 > MR_4^2 > \pi_4 > \pi_4^2$ (Table VII). Additionally, from Eq. [1] it can be seen that $MR_{4'}$, MR_4, π_4, and π_4^2 have a positive influence on the $-\log(IC_{50})$, i.e., decrease inhibitor potency, while σ_4^+, $MR_{4'}^2$, and MR_4^2 enhance inhibitor potency. The negative sign of the 4-position positive Hammet constant (σ_4^+) in Eq. [1] indicates that electron donation from this position promotes inhibitory activity of chalcone oxides. Therefore, the current data set indicates that both steric and electronic effects are important parameters modulating inhibitor potency, which is in contrast with earlier findings (25). Superficially, the hydrophobicity of the position 4-substituent (i.e., π_4) is insignificant; however, its suppression decreases the correlation coefficient to 0.80 and $P(F)$ to 0.58, a finding consistent with previous results (25).

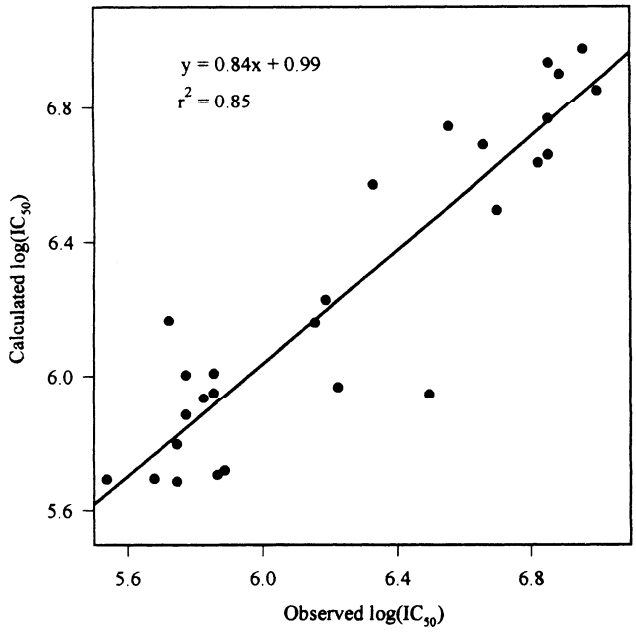

FIG. 1. Predicted vs experimental inhibitor potency.

Three additional inhibitors were synthesized (**48–50**) to test the predictive ability of Eq. [1]. The actual and calculated IC_{50}s for these compounds and four of the excluded carboxylated analogs (calculated for the ionic form) appear in Table V. The QSAR results provided reasonable predictions of potency for good inhibitors ($IC_{50} < 1$ μM) but not for poor ones ($IC_{50} > 50$ μM). Generally, for the carboxylated analogs, methyl esters are predicted to be better inhibitors than free acids. Since a variety of studies predict a hydrophobic region on either side of the catalytic site (5), this result was anticipated. With the exception of 4-phenyl-4′-carboxy chalcone oxide (i.e., **30,** Table V), which showed similar potency to the 4-phenyl-4′-methyl chalcone oxide (**28**), carboxylic acids proved to be much worse inhibitors than predicted by Eq. [1]. It has been hypothesized that in both animals and plants epoxy fatty acids are endogenous substrates of soluble epoxide hydrolase (5). Thus, a properly oriented carboxylic acid functionality may form an ionic or hydrogen bond

TABLE VII

Ranking of QSAR Independent Variables

	$-\log(IC_{50})$	MR_4'	MR_4	π_4	π_4^2	MR_4^2	MR_4^2	σ_4^+
Mean		0.56	0.85	0.027	−0.036	−0.17	−0.21	−0.42
SD[a]	0.22	0.21	0.016	0.07	0.018	0.06	0.09	0.18
b_s[b]		0.53	0.062	0.0086	−0.0029	−0.046	−0.086	−0.34

[a] SD, Standard deviation.

[b] Standardized regression coefficient: $b_s = b_i (S_{xi}/S_y)$, where b_i is the mean regression coefficient of the ith variable. This term represents the predicted increase in y (expressed in standard deviation units of y) expected per standard deviation increase in x. Comparing b_s for each parameter in the multiple regression equation allows a rank order assignment.

in the catalytic sites of both MsEH and HsEH. The greater water solubility of these derivatives may increase their utility in affinity chromatography (35) and as inhibitors for *in vitro* or *in vivo* use.

A similar stepwise development of an equation between the inhibitor structure and the potency of the 27 compounds against HsEH was performed. The resulting correlation was weak ($r \leq 0.67$, $P(F) = 0.06$), indicating that chalcone oxide derivative substituent effects on inhibitor potency with the human enzyme probed with NE2PC were not significant. Nevertheless, the observed relationships appeared to follow the trends observed with the murine enzyme. The use of an analytical substrate with a lower turnover rate (e.g., *trans*-1,2-epoxy-1-(2-quinolyl)pentane (31)) may enhance the ability to discriminate QSAR results with the human enzyme in the future.

Influence of assay conditions on IC_{50}. To verify that the QSAR results were independent of assay conditions and to foster comparisons to previous studies using other sEH activity probes, compounds **1, 2,** and **7** were used to inhibit the hydrolysis of three radioactive substrates (Table VIII). The same rank order of inhibitor potency was observed under all tested conditions. Therefore, the relative IC_{50} appears to be independent of assay conditions and provides a good gauge of inhibitor potency within this class of structural analogs. In MsEH inhibition studies with chalcone oxides using *trans*-β-ethyl styrene oxide and *trans*-stilbene oxide as competitive substrates, chalcone oxides were described as weak inhibitors having higher relative IC_{50}s than those found here (25, 28). It should be noted, however, that a differential increase of IC_{50} values is observed when the incubation time prior to substrate introduction increases (from 5 to 15 min). The increase in IC_{50} is proportional to the rate of inhibitor turnover. Additionally, with potent inhibitors such as **7,** the IC_{50} is depressed by decreasing enzyme concentration (39).

Kinetics of inhibition. To investigate the mechanism of chalcone oxide inhibition, the effects of nine potent inhibitors (**1, 2, 3, 5, 6, 7, 27, 30,** and **36**) on the kinetics of hydrolysis of NE2PC with MsEH and HsEH were examined. Derived kinetic constants are listed in Table IX. Since these inhibitors functioned at concen-

TABLE VIII

Effect of Enzyme Concentration, Incubation Time, and Substrate on IC_{50}[a]

	NEP2C[b]		[^{3}H]t-DPPO[c]	[^{3}H]t-SO[d]	[^{14}C]ESA[c]
K_m (μM)	5.8		2.8	6.0	11.0
k_{cat} (s^{-1})	19.2		26.2	3.3	3.5
[Enzyme] (μM)	0.13		0.003	0.33	0.07
$t_{inc.}$ (min)	5	15	5	5	5
			IC_{50} (μM)[e]		
1	1.7 ± 0.2	6.2 ± 0.6	5 ± 0.3	19 ± 3	50 ± 7
2	1.4 ± 0.5	1.9 ± 0.1	1.8 ± 0.1	8 ± 1	8 ± 1
7	0.13 ± 0.02	0.15 ± 0.01	0.027 ± 0.001	0.44 ± 0.05	0.10 ± 0.03

[a] All enzymes were incubated with inhibitors for $t_{inc.}$ min in pH 7.4 phosphate buffer 0.1 M at 30°C prior to substrate introduction.

[b] Hydrolysis of 4-nitrophenyl-*trans*-2,3-epoxy-3-phenylpropyl carbonate was assayed according to Dietze *et al.* (31).

[c] Hydrolysis of *trans*-[^{3}H]diphenylpropene oxide and [^{14}C]epoxy steric acid was assayed according to Borhan *et al.* (38).

[d] Hydrolysis of *trans*-[^{3}H]stilbene oxide was assayed according to Wixtrom and Hammock (7).

[e] Mean ± standard deviation ($n = 3$).

TABLE IX

Kinetic Constants for MsEH and HsEH Inhibition

	Mouse sEH				Human sEH			
No.	K_d (μM)[a]	k_2 (s^{-1})[a]	k_3 (10^{-4} s^{-1})[b]	$t_{1/2}$ (min)	K_d (μM)[a]	k_2 (s^{-1})[a]	k_3 (10^{-4} s^{-1})[b]	$t_{1/2}$ (min)
1	0.92 ± 0.17	0.15 ± 0.01	60 ± 8	1.9	4.1 ± 0.7	0.29 ± 0.03	29 ± 1	4.0
2	1.2 ± 0.5	0.20 ± 0.05	62 ± 4	1.9	1.5 ± 0.3	0.32 ± 0.04	22 ± 3	5.3
3	0.20 ± 0.05	0.09 ± 0.01	28 ± 3	4.2	0.6 ± 0.1	0.22 ± 0.03	21 ± 2	5.5
5	0.74 ± 0.07	0.50 ± 0.03	9.9 ± 0.6	11.7	0.90 ± 0.05	0.65 ± 0.03	6.9 ± 0.6	16.8
6	0.27 ± 0.04	0.06 ± 0.01	64 ± 2	1.8	0.36 ± 0.08	0.14 ± 0.02	37 ± 1	3.1
7	0.43 ± 0.07	0.36 ± 0.04	8.8 ± 0.4	13.1	0.45 ± 0.05	0.56 ± 0.04	6.2 ± 0.4	18.7
27	0.27 ± 0.08	0.24 ± 0.04	8.8 ± 0.3	13.1	0.54 ± 0.11	0.42 ± 0.06	5.0 ± 0.4	23.1
30	0.76 ± 0.02	0.46 ± 0.09	8.2 ± 0.5	14.1	0.75 ± 0.11	0.56 ± 0.06	6.4 ± 0.2	18.1
36	0.77 ± 0.10	0.65 ± 0.17	14.0 ± 1.0	8.3	0.97 ± 0.13	0.75 ± 0.13	9.0 ± 0.3	12.8

[a] The nonlinear regression of the initial rate of EC formation (ρ) versus inhibitor concentration ([I]) permits the calculation of K_d and k_2 according to Eq. [3]. Value ± 95% confidence interval.

[b] The slope of EC complex decomposition, ln (A_0 − A) versus time, permits the calculation of k_3 according to Eq. [4]. Mean ± standard deviation (n = 3).

trations near that of the enzyme target (Table I) Michaelis–Menten kinetics (40) could not be used. Fast-gel filtration (Bio-Spin column P-30; Bio-Rad, Hercules, CA) of a 1:1 mixture of MsEH and compound **7** permitted the recovery of less than 10% of enzyme activity, indicating a strong liaison between the inhibitor and the enzyme. Moreover, the time course of sEH inhibition by compounds **1, 2,** and **7** was bimodal with a rapid increase in inhibition during the first minute followed by gradual enzyme recovery, which was complete given sufficient time (20 to 60 min—results not shown). Inhibitor decomposition in the absence of enzyme was less than 5% after 24 h. Therefore the kinetic results obtained were considered to reflect enzymatic hydrolysis only. These results indicate an irreversible inhibition of sEH by chalcone oxides through the formation of a covalent intermediate and slow enzyme reactivation transforming the inhibitor to an inactive product. Additionally, the rapid depletion of inhibitors working at stoichiometric concentrations would suggest that K_d is a tight binding event as described by Morisson (41). While slow-tight binding kinetics have been used to describe the inhibition of hydrolytic enzymes (42), their use is only appropriate when inhibition proceeds from a single kinetic event. Irreversible inhibition of a multistep enzymatic process has been described for the action of carbamates and organophosphates on acetylcholinesterases by Main (36) using

$$E + I \underset{}{\overset{K_d}{\rightleftharpoons}} EI \xrightarrow{k_2} EC \xrightarrow{k_3} E + P, \qquad [2]$$

where E, I, and P are, respectively, the enzyme, inhibitor, and inactive product; K_d is the dissociation constant of the complex EI; k_2 is the first-order formation rate of the covalent enzyme–inhibitor complex EC (an irreversible step); and k_3 is the first-order decomposition rate of EC to yield the reactivated enzyme E and released inactive product P.

To calculate K_d and k_2 while minimizing the effect of k_3, activity was measured at multiple time points immediately after inhibitor addition ($t \ll t_{1/2}$), allowing determinations of the initial rate of EC formation at t_0 (ρ) by extrapolation. This value is described by

$$\rho = \frac{\ln \dfrac{[E_T]}{([E_T] - [EC])}}{t} = \frac{ln\left(\dfrac{A_{t=0}}{A_t}\right)}{t} = \frac{k_2[I]}{[I] + K_d}. \qquad [3]$$

The plot of ρ versus [I] (Fig. 2A) permitted the calculation of K_d and k_2 (Table IX).

The rate of EC degradation is described by

$$\ln [EC] = \ln (A_{t=0} - A_t) = -k_3 t + c. \qquad [4]$$

A plot of ln (A_0 −A) versus time (Fig. 2B) allowed the calculation of k_3. Using k_3, the half-life of the enzyme–inhibitor complex was calculated directly.

The accuracy of the applied kinetic model was assessed by comparing theoretical and measured results for ρ; correlation factors >0.95 were found. The results in Table IX indicate that both enzymes display similar variations in their kinetic parameters, suggesting a consistent mechanism of inhibition. The inhibitors studied exhibited affinity constants, i.e., K_ds, between 2 and 10 times the enzyme concentration, supporting a tight binding component of inhibition. Main kinetics

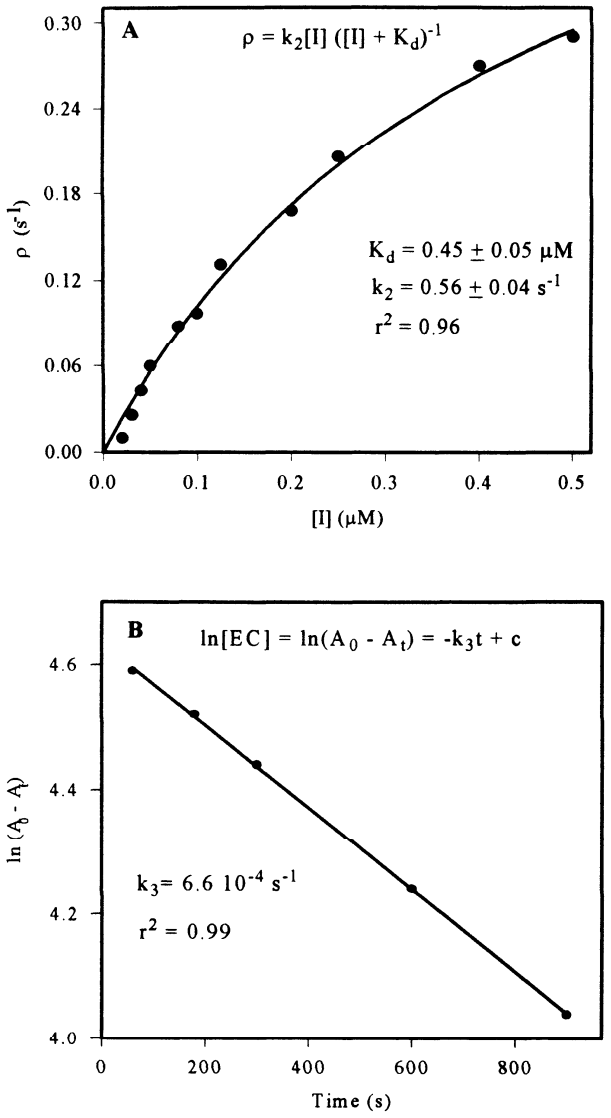

FIG. 2. Determination of kinetic constants of human sEH inhibition by compound **7**. Human soluble epoxide hydrolase (0.26 μM) was incubated at 30°C in 0.1 M sodium phosphate buffer at pH 7.4 containing 0.1 mg/ml of BSA and 1% of dimethyl formamide. (A) Kinetics of EC complex formation: initial rate of EC formation (ρ) versus inhibitor concentration [I]. This nonlinear regression permits the calculation of K_d and k_2 according to Eq. [3]. (B) Kinetics of EC complex decomposition: ln (A_0 − A) versus time. The slope permits the calculation of k_3 according to Eq. [4].

(36) assumes that [I] ≫ [E] and [S] is sufficiently large to ensure complete dissociation of EI. Since many of these compounds approach stoichiometric inhibition, [I] is not always ≫ [E]; however, considering the fastest inhibitor turnover, the [I] will decrease by less than 10% of its initial concentration during the experimental time course. Based on experimental inhibitor and substrate concentrations, a maximal error in observed K_d of ~5% can be attributed to incomplete dissociation of EI. The degradation rates of the EC complexes for the tested inhibitors were 25- to 1000-fold slower than their rates of formation (k_2/k_3), supporting the hypothesis that chalcone oxides inhibit sEH by forming stabilized alkyl–enzyme intermediates. Moreover, this value indicates a 4% maximal error in k_2 due to the EC degradation. Similarly, the dealkylation of the alkyl–enzyme intermediate between microsomal EH and good substrates was recently shown to be rate limiting (43).

Structural changes at positions 4 (**1–7**) and 4′ (**27** and **30**) and on the γ-carbon (**36**) were not correlated with K_d. The nature of the position 4 (**1** to **7**) substitution had the dominant influence on the rate of alkyl–enzyme formation (k_2). The Hammet plot (Fig. 3) showing the logarithm of the relative rates ($^{4\text{-R}}k_2/^{4\text{-H}}k_2$) versus the constant $\sigma+$ for each 4-position substituent illustrates this influence. The linear relationship (r^2 = 0.87) observed for both enzymes indicates a consistent mechanism operating throughout the chalcone oxide series. The ketone of compound **1** induced an approximate 4000-fold decrease in the rate of alkyl–enzyme intermediate decomposition (k_{cat}/k_3) compared to the structurally related *trans*-1,3-diphenylpropene oxide (t-DPPO), a good sEH substrate (38; Table VIII). The EC complex stabilizing effects of the γ-carbon ketone relative to the γ-carbon hydroxyl (**7** vs **36**) indicates the importance of a polarizable function at this position. As with esterases, other members of the α/β-hydrolase fold family (44), increasing the hydrophobicity of the

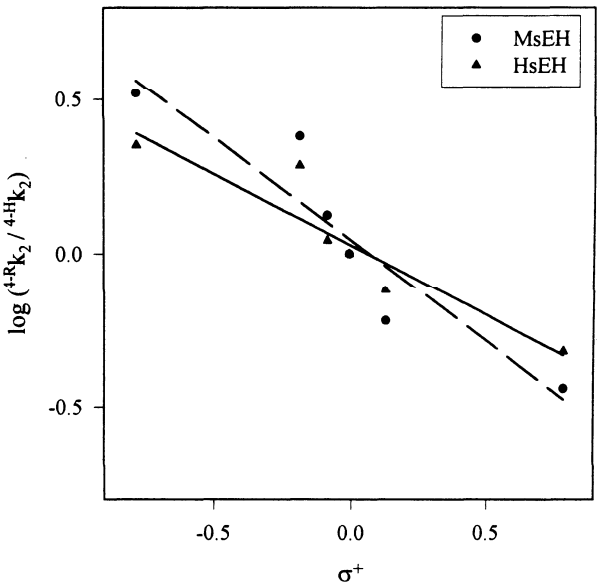

FIG. 3. Log of the sEH–inhibitor complex relative rate of formation ($^{4\text{-R}}k_2/^{4\text{-H}}k_2$) for *para*-substituted chalcone oxides versus σ^+, the positive Hammet constant.

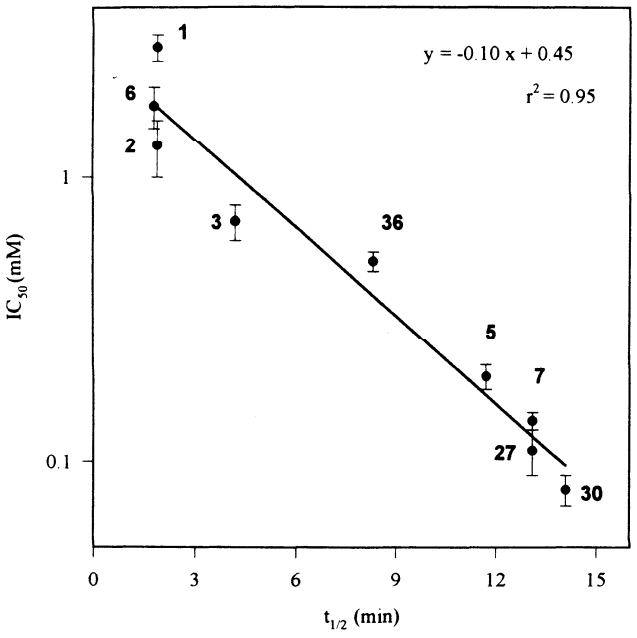

FIG. 4. Inhibitor potency [$-\log(IC_{50})$] versus enzyme–inhibitor complex half-life for the MsEH.

substrate decreased the deacylation rate, thereby increasing the time to reactivation (e.g., **1** vs **7**, Table IX).

Regression of the EC complex half-life with respect to the log IC_{50} of the murine sEH showed a strong correlation (r^2 = 0.95; Fig. 4), indicating that the inhibitory potency is dominated by k_3. Therefore the described structure–activity relationship of inhibition potency is inversely related to the speed of enzyme reactivation (k_3). While a similar correlation was not observed for HsEH ($r^2 \leq 0.3$), the low variability in inhibition of this enzyme with the tested structural analogs as detected using NE2PC may have prevented this discrimination.

DISCUSSION

The overall mechanism of epoxide hydrolysis by sEH and mEH has recently been elucidated (21–24). As with other members of the α/β-hydrolase fold family of enzymes (21, 45), EHs have a two-step mechanism. Using the amino acid numbers from the murine sEH, first the reactive nucleophile Asp^{333} attacks the oxirane ring, leading to ring opening and formation of a hydroxylalkyl enzyme. In the second step the covalent intermediate is hydrolyzed by a His^{523}–Asp^{495}-activated water. The rapid reactivation of a recombinant Asn^{333} mutation to a functional Asp^{333} (46) provides convincing evidence for the presence of a strongly basic water molecule in the catalytic site prior to substrate binding (Fig. 5A). The time-dependent inhibition with slow recovery observed with chalcone oxide inhibition of both the murine and the human enzyme is consistent with the formation of a covalent intermediate, which reacts slowly to liberate a nonactive product (Fig. 5A). For aryl carbamate inhibition of cholesterol esterase, another α,β-fold hydrolase enzyme (47), the inhibitory potency increases progressively as the molecular volume of the aromatic fragment is increased (48) and steric parameters influence the decarbamylation rate (k_3) of the enzyme–inhibitor complex. A similar effect is observed for the chalcone oxide inhibition of soluble epoxide hydrolases, suggesting the existence of steric constraints during the EH catalytic cycle.

Inhibitor potencies as described by the IC_{50}s are functionally dependent on assay conditions and are composites of kinetic constants when considering multistep enzymatic mechanisms. Therefore to fully describe the inhibitory mechanism, the rates of binding, acylation, and deacylation need to be considered separately. Unfortunately, irreversible inhibitors such as chalcone oxides do not cause a permanent enzyme inactivation. Rather, irreversible inhibition describes a system in which neither the active enzyme nor the inhibitor can be recovered. Since chalcone oxides are actually sEH substrates, bad inhibitors are likely to have k_3 and k_2 values which are close, violating the kinetic model of Main (36). Therefore, QSAR analysis based on IC_{50} data effectively focused kinetic investigations onto the most active compounds within the large screening battery, simplifying the resulting interpretations and preventing erroneous comparisons using an inappropriate kinetic model. Conditions for determining IC_{50} which resulted in maximal and steady-state inhibition and negligible reactivation were selected.

The finding that the IC_{50} was directly related to the half-life of the MsEH intermediate complex (Fig. 4) provided a mechanistic argument supporting the QSAR results. The QSAR analysis identified optimal steric constraints and supported a mechanism of inhibition consistent with electronic stabilization of an enzyme–inhibitor intermediate. The 4- and 4′-positions were found to have optimal steric constraints on substitution bulk to an *n*-pentyl (or phenyl) or *n*-propyl group, respectively. Additionally, the presence of hydrophobic moieties at position 4 strengthened inhibition while neither the charge state ($\sigma_{4'}^{+}$) nor the hydrophobicity of the 4′-position appeared to influence the inhibitory potency of the chalcone oxides examined here. Using a set of nine 4-substituted (**1–7, 12,** and **14**) and eight 4′-substituted chalcone oxides (**1, 16, 17,** and **20–23**) Mullin and Hammock developed two independent structure–activity relationships for the effects of structural modifications at the 4- and 4′-positions (25). These workers, unaware of the two-step sEH catalytic mechanism, used a Lineweaver–Burk approach and

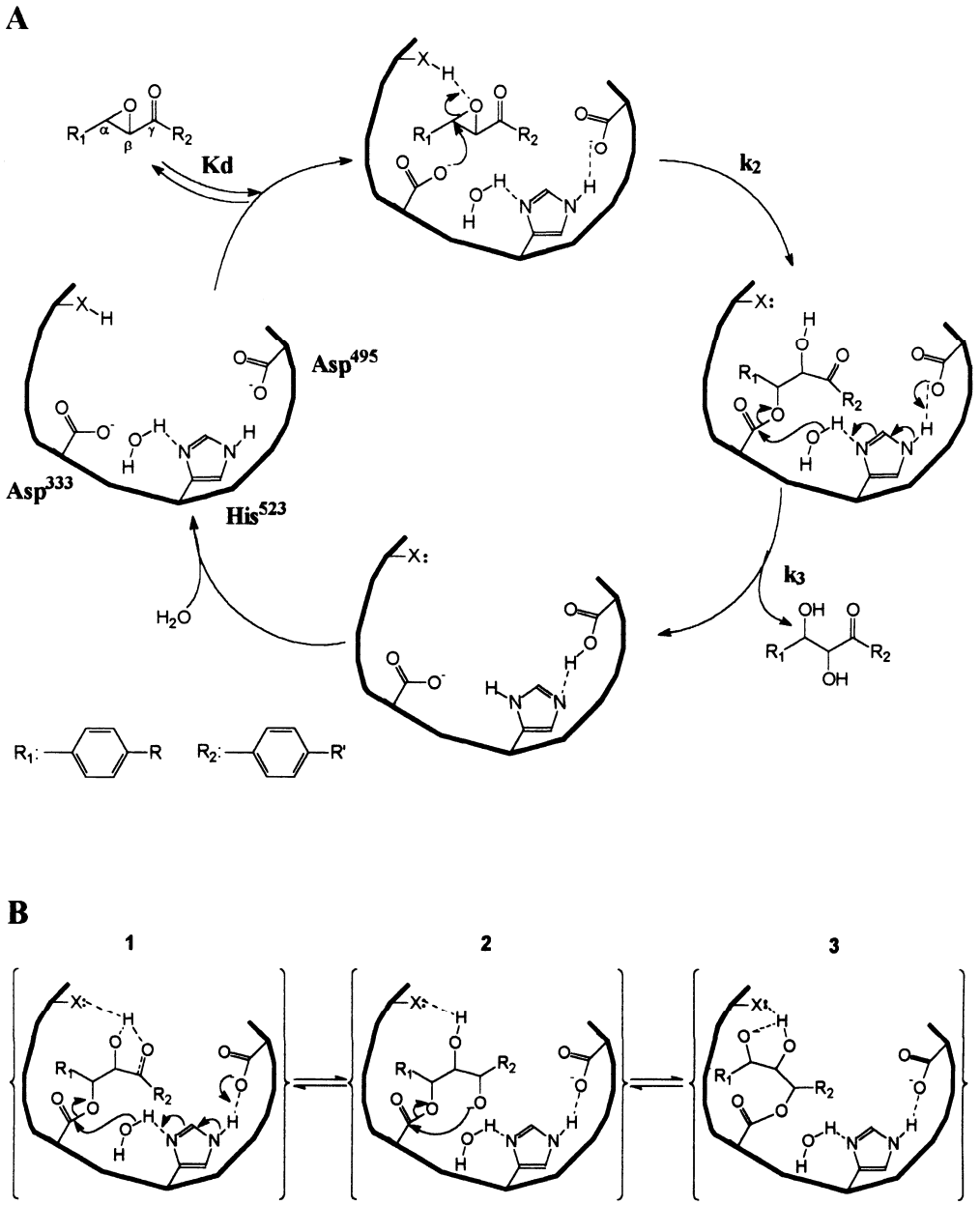

FIG. 5. Proposed mechanism of sEH inhibition by chalcone oxides. (A) sEH catalytic cycle. (B) Proposed structures of the stable enzyme–inhibitor complex (EC).

their results strongly suggested slow-tight binding kinetics as developed by Morrison (41). These findings are consistent with our detection of a tight binding component in the inhibitory mechanism. Contrary to our findings, however, Mullin and Hammock determined substituent effects on inhibitor behavior to be dominated by hydrophobic terms with modulation by 4-position molecular refractivity and 4′-steric, but not electronic, parameters (25). By expanding the tested series to include numerous structural analogs with divergent electronic properties, fusing the mathematical treatment of the 4- and 4′-substitution, and using Main kenetics, we have detected both steric and electronic parameters as modulators of inhibitor potency.

The effects of the 4-position electronic characteristics on the rate of hydroxylalkyl enzyme formation (k_2) have been analyzed using a Hammet plot (Fig. 3). The Hammet parameter (i.e., the slope) for each

enzyme was small, i.e., −0.66 and −0.46 for MsEH and HsEH, respectively. The negative correlation indicates the development of a positive charge at the reactive center in the "early" transition state structure of epoxide opening. Additionally, the magnitude of the Hammet parameter suggests a weak charge which excludes the formation of a true carbonium ion and which is consistent with previous suggestions (5). In the classical acid-catalyzed hydration of aromatic epoxides the Hammet parameter is 10-fold higher yet retains a negative slope, e.g., −4.2 for styrene oxide derivatives (49). The weak Hammet parameter is consistent with an electron-donating group at the 4-position of the α-phenyl moiety inducing the stabilization of a relative positive charge on the transition state α-carbon. This then suggests a push–pull mechanism, in which the epoxide oxygen is activated by protonation, weakening the C–O epoxide bond and facilitating a nucleophilic attack on the α-carbon by the Asp^{333} carboxylate anion. This hypothesis fits the regioselectivity of sEH hydrolysis of t-DPPO (22) and *trans*-1-phenylpropene oxide (50) which occurs on the α-carbon. Free carboxylic acids are weak, hard nucleophiles which are not expected to easily open epoxide rings. One anticipates, however, that the microenvironment of the catalytic site transforms Asp^{333} into a soft base of increased nucleophilicity. Coordination of an epoxide oxygen with a Lewis acid is known to chemically activate epoxide carbons toward attack by weak nucleophiles (51). Based on sequence analogy and directed mutagenesis, a few amino acids have been proposed to activate the epoxide by hydrogen bonding with the oxirane oxygen (23, 52, 53). Therefore, a γ-carbon carbonyl may compete with the epoxide for hydrogen bonding, resulting in a decreased speed of intermediate formation. This hypothesis is consistent with the approximate 2-fold increase in k_2 observed when the ketone of **7** was reduced, forming the corresponding glycidol, **36.**

The slow hydrolysis of the phenyl chalcone oxide glycidol analog (**36,** Table IX) is consistent with the reported inhibition of sEH by 3-*trans*-phenylglycidol (29, 30) and suggests that glycidol sEH inhibition also proceeds from a stabilized enzyme–inhibitor complex (Fig. 5). Comparing glycidols with the corresponding chalcone oxides tested (**33–1, 34–2, 35–6, 36–7,** and **37–28**) revealed a decline in inhibitory potency associated with the reduction of the chalcone oxide γ-carbonyl. Glycidol-induced inhibition was not, however, enhanced appreciably by electron-donating *para*-substituents on the α-carbon phenyl (**33–37,** Table IV). The differential 4-position electronic effect on inhibitor potency in the chalcone oxide and glycidol series suggests a different acylation regioselectivity through the glycidol series. This hypothesis is supported by the 80% incorporation of ^{18}O from water at the β-carbon of some (*S,S*)-*trans*-3-phenylglycidols (29) rather than the α-carbon attack suggested for the chalcone oxides.

Numerous investigations into sEH substrate selectivity indicate that the enzyme can be viewed as having a hydrophobic binding site on either side of the catalytic site. Thus the chalcone oxides with chirality at the α- and β-carbons can be envisioned as lying in the catalytic site with the 4-position to the "left" or to the "right" and with the epoxide either "up" or "down." Chalcones with small *para*-substitutions show little enantioselectivity in inhibitory potency (29). The differences in steric constraints identified for the 4- and 4′-positions suggest that chalcone oxides with larger substitutions have reduced freedom in docking such that epoxide orientation will become the sole enantioselective trait. Under these conditions, the overall enzymatic mechanism should not be altered but relative rates and regioselectivity of nucleophilic attack may be altered. Further studies on the enantioselectivity of phenyl-substituted chalcone oxide inhibitors are therefore suggested.

Several hypotheses have been described to explain the influence of substitutions at the 4-position and the γ-carbon of chalcone oxides on the stabilization of the intermediate complex (22, 25). The γ-carbon ketone enhancement of inhibitor potency has many possible explanations. The ketone may interfere with the epoxide binding in the "oxyanion hole" preventing polarization of the carbon–oxygen bond of the epoxide. However, one would expect such interaction to dramatically reduce the formation of the alkyl enzyme (k_2) much more than turnover or reactivation (k_3) and this was not observed. Interactions between the γ-ketone and the catalytic water may reduce the nucleophilic character of this activated water molecule, reducing its propensity to attack the alkylated carboxylate of Asp^{333}. Alternatively, enolization of the ketone would allow for a direct interaction between the enol and the catalytic water molecule (Fig. 5B2). Additionally, in this situation the enolate and water molecule would compete for the electrophilic center of the alkylated Asp^{333}, thus reducing the rate of deacylation (Fig. 5B2). An intramolecular attack of the γ-enol on the Asp^{333} could break the covalent bond with the α-carbon of the chalcone oxide while forming a new bond between Asp^{333} and the γ-hydroxyl, generating a new covalent intermediate complex (Fig. 5B3). The presence of a position-4 electron-donating group should enhance the formation and stability of the covalent intermediates shown in Fig. 5B1, decreasing the susceptibility of the resulting acyl enzyme to hydrolytic attack. This agrees with the observed mechanism of sEH (23) and supports the hypothesis that chalcone oxides act as alternative substrates which are slowly

hydrolyzed due to electronic stabilization of the acyl enzyme intermediate.

Herein fortifying IC_{50}s with kinetic descriptions, we have improved our understanding of the mechanism of sEH inhibition by chalcone oxides. The sample size was insufficient to discern an association between linear free energy parameters and K_d. The importance of resonance effects on the IC_{50} suggests that 4-position electron-donating groups enhance the speed of alkylation and possibly decrease the rate of dealkylation. The dominance of k_3 on IC_{50} supports the hypothesized enzyme–inhibitor complex stabilization. Moreover, chalcone oxides and glycidols appear to have similar, yet distinct mechanisms of inhibition. These findings will aid in the design of mechanism-based irreversible inhibitors of this enzyme and have defined the boundaries for future kinetic studies. Additionally, while murine and human enzymes showed differential susceptibility to the investigated inhibitors, the underlying mechanisms appeared equivalent. Therefore, mice seem to be a reasonable model for the development of human soluble epoxide hydrolase inhibitors.

ACKNOWLEDGMENTS

We thank Dr. M. Goodrow and Dr. J. Zheng for their helpful discussions in the synthesis and Dr. Y. Nakagawa of the Department of Agricultural Chemistry, Kyoto University, for his helpful comments and assistance in the QSAR multiple regression analysis.

REFERENCES

1. Oesch, F. (1972) *Xenobiotica* **3,** 305–340.
2. Watabe, T., Kanai, M., Isobe, M., and Ozawa, N. (1981) *J. Biol. Chem.* **256,** 2900–2907.
3. Rädmark, O., Shimizu, T., Jörnvall, H., and Samuelsson, B. (1984) *J. Biol. Chem.* **259,** 12339–12345.
4. Pace-Asciak, C. R., and Lee, W. S. (1989) *J. Biol. Chem.* **264,** 9310–9313.
5. Hammock, B. D., Grant, D., and Storms, D. (1997) *in* Comprehensive Toxicology (Sipes, I., McQueen, C., and Gandolfi, A., Eds.), Chap. 18, pp. 283–305, Pergamon, Oxford.
6. Meijer, J., and DePierre, J. W. (1988) *Chem. Biol. Int.* **64,** 207–249.
7. Wixtrom, R. N., and Hammock, B. D. (1985) *in* Biochemical Pharmacology and Toxicology (Zakim, D., and Vessey, D. A., Eds.), Vol. 1, pp. 1–93, Wiley, New York.
8. Zeldin, D. C., Wei, S., Falck, J. R., Hammock, B. D., Snapper, J. R., and Capdevila, J. H. (1995) *Arch. Biochem. Biophys.* **316,** 443–451.
9. Zeldin, D. C., Moomaw, C. R., Jesse, N., Tomer, K. B., Beetham, J., Hammock, B. D., and Wu, S. (1996) *Arch. Biochem. Biophys.* **330,** 87–96.
10. Moghaddam, M., Grant, D., Cheek, J., Greene, J. F., Williamson, K. C., and Hammock, B. D. (1997) *Nat. Med.* **3,** 562–566.
11. McGiff, J. C., Steinberg, M., and Quilley, J. (1996) *Trends Cardiovasc. Med.* **6,** 4–10.
12. Ozawa, T., Hayakawa, M., Takamura, T., Sugiyama, S., Suzuki, K., Iwata, M., Taki, T., and Tomita, T. (1986) *Biochem. Biophys. Res. Commun.* **137,** 1071–1078.
13. Sevanian, A., Mead, J. F., and Stein, R. A. (1978) *Lipids* **14,** 634–643.
14. Ishizaki, T., Shigemori, K., Ameshima, S., Nakai, T., Miyabo, S., Hayakawa, M., Ozawa, T., and Voelkel, N. F. (1996) *Am. J. Physiol.* **271,** L459–L463.
15. Ozawa, T., Hayakawa, M., Kosaka, K., Sugiyama, S., Ogawa, T., Yokoo, K., Aoyama, H., and Izawa, Y. (1990) *Adv. Prostaglandin. Thromboxane Leukotriene Res.* **21,** 569–572.
16. Dudda, A., Spiteller, G., and Kobelt, F. (1996) *Chem. Phys. Lipids* **82,** 39–51.
17. Sakai, A., Ishizaki, T., Onishi, T., Sasaki, F., Ameshma, S., Nakai, T., Miyabo, S., Matsukawa, S., Hayakawa, M., and Ozawa, T. (1995) *Am. J. Physiol.* **269,** L326–L331.
18. Fukushima, A., Hayakawa, M., Sugujama, S., Ajioka, M., Ito, T., Satake, T., and Ozawa, T. (1988) *Cardiovasc. Res.* **22,** 213–218.
19. Ishizaki, T., Shigemuri, K., Nakai, T., Miyabo, S., Ozawa, T., Chang, S., and Voekel, N. F. (1995) *Am. J. Physiol.* **269,** L65–L70.
20. Grant, D. F., Greene, J. F., Pinot, F., Borham, B., Moghaddam, M. F., Hammock, B. D., McCuthen, B., Ohkama, H., Luo, G., and Guenthner, T. M. (1996) *Biochem. Pharmacol.* **51,** 503–515.
21. Beetham, J. K., Grant, D., Arand, M., Garbarino, J., Kiyosue, T., Pinot, F., Oesch, F., Belknap, W. R., Shinozaki, K., and Hammock, B. D. (1995) *DNA Cell Biol.* **14,** 61–71.
22. Borhan, B., Jones, A. D., Pinot, F., Grant, D. F., Kurth, M. J., and Hammock, B. D. (1995) *J. Biol. Chem.* **270,** 26923–26930.
23. Arand, M., Wagner, H., and Oesch, F. (1996) *J. Biol. Chem.* **271,** 4223–4229.
24. Lacourciere, G. M., and Armstrong, R. N. (1993) *J. Am. Chem. Soc.* **115,** 10466–10467.
25. Mullin, C. A., and Hammock, B. D. (1982) *Arch. Biochem. Biophys.* **216,** 423–429.
26. Meijer, J., and DePierre, W. (1985) *Eur. J. Biochem.* **150,** 7–16.
27. Dietze, E. C., Stephens, J., Magdalou, J., Bender, D. M., Moyer, M., Fowler, B., and Hammock, B. D. (1993) *Comp. Biochem. Physiol.* **104B,** 2999–3008.
28. Miyamoto, T., Silva, M., and Hammock, B. D. (1987) *Arch. Biochem. Biophys.* **254,** 203–213.
29. Dietze, E. C., Kuwano, E., Casas, J., and Hammock, B. D. (1991) *Biochem. Pharmacol.* **42,** 1163–1175.
30. Dietze, E. C., Casas, J., Kuwano, E., and Hammock, B. D. (1993) *Comp. Biochem. Physiol.* **104B,** 309–314.
31. Dietze, E. C., Kuwano, E., and Hammock, B. D. (1994) *Anal. Biochem.* **216,** 176–187.
32. Adam, W., Bialas, J., and Hadjiarapoglou, L. (1991) *Chem. Ber.* **124,** 2377.
33. Grant, D. E., Storms, D. H., and Hammock, B. D. (1993) *J. Biol. Chem.* **268,** 17628–17633.
34. Beetham, J. K., Tian, T., and Hammock, B. D. (1993) *Arch. Biochem. Biophys.* **305,** 197–201.
35. Wixtrom, R. N., Silva, M. H., and Hammock, B. D. (1988) *Anal. Biochem.* **169,** 71–80.
36. Main, A. R. (1982) *in* Introduction to Biochemical Toxicology (Hodgson, E., and Guthrie, F. E., Eds.), pp. 193–223, Elsevier, New York.
37. Hansch, C., and Leo, A. (1979) Substituent Constants for Correlation Analysis in Chemistry and Biology, Wiley, New York.

38. Borhan, B., Mebrahtu, T., Nazarian, S., Kurth, M. J., and Hammock, B. D. (1995) *Anal. Biochem.* **231,** 188–200.
39. Hammock, B. D., Prestwich, G. D., Loury, D. N., Cheung, P. Y. K., Eng, W-S., Park, S-K., Moody, D. E., Silva, M. H., and Wixtrom, R. N. (1986) *Arch. Biochem. Biophys.* **244,** 292–309.
40. Segel, I. H. (1975) *in* Enzyme Kinetics, Behavior and Analysis of Rapid Equilibrium and Steady-State Enzyme Systems, pp. 100–226, Wiley, New York.
41. Morrison, J. F. (1982) *Trends Biochem. Sci.* **7,** 102–105.
42. Abdel-Aal, Y. A. I., and Hammock, B. D. (1985) *Insect Biochem.* **15,** 111–122.
43. Tzeng, H-F., Laughlin, T., Lin, S., and Armstrong, R. N. (1996) *J. Am. Chem. Soc.* **118,** 9436–9437.
44. Huang, T. L., Shiotsuki, T., Uematu, T., Borhan, B., Li, Q. X., and Hammock, B. D. (1996) *Pharmacol. Res.* **13,** 1495–1500.
45. Verschueren, K. H. G., Seljée, F., Rozeboom, H. J., Kalk, K. H., and Dijkstra, B. W. (1993) *Nature* **363,** 693–698.
46. Pinot, F., Grant, D. F., Beetham, J. K., Parker, A. G., Borhan, B., Land, S., Jones, A. D., and Hammock, B. D. (1995) *J. Biol. Chem.* **270,** 7968–7974.
47. Ollis, D. L., Cheah, E., Cygler, M., Dijkstra, B., Frolow, F., Franken, S. M., Harel, M., Remington, S. J., Silman, I., Schrag, J., Sussman, J. L., Vershueren, K. H., and Goldman, A. (1992) *Protein Eng.* **5,** 197–211.
48. Feaster, S. R., Lee, K., Baker, N., Hui, D. Y., and Quinn, D. M. (1996) *Biochemistry* **35,** 16723–16734.
49. Blumenstein, J. J., Ukachukwu, V. C., Mohan, R. S., and Whalen, D. L. (1993) *J. Org. Chem.* **58,** 924–932.
50. Bellucci, G., Chiappe, C., and Berti, A. (1994) *Tetrahedron Lett.* **35,** 4219–4222.
51. Parker, R. E., and Isaacs, N. S. (1959) *Chem. Rev.* 737–799.
52. Arand, M., Grant, D. F., Beetham, J. K., Friedberg, T., Oesch, F., and Hammock, B. D. (1994) *FEBS Lett.* **338,** 251–256.
53. Bell, P. A., and Kasper, C. B. (1993) *J. Biol. Chem.* **268,** 14011–14017.